Analytical expression for large signal transfer function of an optically filtered analog link

T. Banwell, A. Agarwal, P. Toliver, J. Jackel, and T.K. Woodward

Telcordia Technologies, Red Bank, New Jersey 07701
bct@research.telcordia.com

Abstract: We present an analytical expression for the transfer function of an *optically-filtered* radio frequency photonic link using phase modulation and coherent detection. This solution is applicable to quadrature passband signals and is significant for evaluating the distortion and consequently improving the linearity of such electrical-optical-electrical links. We show that the nonlinearity appears as an envelope distortion and discuss linearization techniques along with experimental validation.

OCIS codes: (060.2330) Fiber optics communications; (060.5625) Radio frequency photonics.

References and links

1. C. Cox, *Analog Optical Links*, (Cambridge University Press, Cambridge, U.K., 2004).
2. W. S. C. Chang, *RF photonic technology in optical fiber links*, (Cambridge University Press, Cambridge, U.K., 2002).
3. M. Nazarathy, J. Berger, A. J. Ley, I. M. Levi, and Y. Kagan, "Progress in externally modulated AM CATV transmission systems," J. Lightwave Technol. **11**(1), 82–105 (1993).
4. G. E. Betts, "Linearized modulator for suboctave-bandpass optical analog links," IEEE Trans. Microw. Theory Tech. **42**(12), 2642–2649 (1994).
5. L. M. Johnson, and H. V. Roussell, "Reduction of intermodulation distortion in interferometric optical modulators," Opt. Lett. **13**(10), 928–930 (1988).
6. J. Zhang, and T. E. Darcie, "Two-tone analysis of distortion suppression in microwave photonic links using phase modulation and fiber-Bragg grating filters," International Symposium on Signals, Systems and Electronics, Montreal, Quebec, 2007.
7. A. Ramaswamy, L. A. Johansson, J. Klamkin, H.-F. Chou, C. Sheldon, M. J. Rodwell, L. A. Coldren, and J. E. Bowers, "Integrated coherent receivers for high-linearity microwave photonic links," J. Lightwave Technol. **26**(1), 209–216 (2008).
8. T. R. Clark, and M. L. Dennis, "Coherent optical phase modulation link," IEEE Photon. Technol. Lett. **19**(16), 1206–1208 (2007).
9. I. S. Gradshteyn, and I. M. Ryzhik, *Table of Integral Series and Products*, (Academic Press, San Diego, Calif., 1994), pp. 979.
10. A. Agarwal, T. Banwell, J. Jackel, P. Toliver, and T. K. Woodward, "Multiscale Sampling for Wide Dynamic Range Electro-optic Receivers," *Optical Fiber Communication*, (Optical Society of America, San Diego, USA, 2009), OMI3.

1. Introduction

Microwave photonic links have been studied extensively due to their growing applications at high frequencies in commercial and defense communications such as CATV, antenna remoting, avionics, synthetic aperture radar, phased array antenna etc [1,2]. Radio frequency (RF) photonics is attractive for both transmission and signal processing. RF signal processing applications such as channelizing receivers provide the opportunity for optics to transform the challenging task of wideband spectral processing at high frequencies in the RF domain to narrowband processing in the optical domain with reduced complexity.

The utility of analog links depends upon various parameters including link gain, noise figure, bandwidth, and link linearity or dynamic range. High dynamic range is key to achieving high fidelity analog links and places highly challenging requirements on the components and the design of the system. The linearity of the link can be characterized by the spurious free dynamic range (SFDR) and is primarily dependent on the modulation and detection scheme. Both intensity modulation using direct detection and phase modulation using either direct detection or coherent detection have been studied. All these links exhibit a

#112111 - $15.00 USD Received 1 Jun 2009; revised 5 Aug 2009; accepted 13 Aug 2009; published 17 Aug 2009

nonlinear transfer function and are thus limited in their linearity. Besides modulation and detection, the characteristic of the nonlinearity also depends on whether the link employs filtering.

Both optical and electronic methods to extend the dynamic range have been proposed and demonstrated. Electronic methods involve electronic predistortion [3] while optical methods include cascaded modulators for predistortion [4,5], optical spectrum shaping [6], optical phase locked loops (PLL) [7], and coherent post-processing [8]. Significant reduction in the intermodulation distortion has been achieved using these methods. Predistortion techniques require knowledge of the nonlinearity and may employ adaptive circuits to track changes in the input signal. Post-processing methods are extensively used in applications such as software defined radio (SDR). However, the post-processing methods such as an electro-optical PLL demonstrated so far rely on having access to the entire modulated signal in order to compensate for link nonlinearity and reconstruct the original transmitted signal.

In this paper we consider a filtered microwave photonic link useful for signal processing applications where the RF signal and the optical IF signal have the same bandwidth. We present an exact analytical solution for the transfer function of a phase-modulated passband filtered analog photonic link using balanced coherent detection. Of note is that this analysis is valid for both small and large passband RF signals. We present experimental time domain results from a two-tone test that confirms this analysis. Based on knowledge of the generic transfer function we present predistortion and post-processing techniques for linearization even when only a single sideband of the modulated signal band is accessible at the receiver.

2. Quadrature signals

Many RF waveforms that might be subjected to optical signal processing can be characterized by a center frequency ω_{RF} and a bandwidth Δ. Such passband signals can be expressed in terms of an RF carrier and two quadrature components $x(t)$ and $y(t)$ as

$$z(t) = x(t)\sin(\omega_{RF}t) + y(t)\cos(\omega_{RF}t) \tag{1}$$

Information is carried by the quadrature modulation components. The quadrature components for some common waveforms are listed in Table 1.

Table 1. Quadrature representation of some common RF waveforms

SIGNAL	***x(t)***	***y(t)***
SINGLE SIDEBAND	$x(t)$	$\tilde{x}(t) = \frac{1}{\pi}\int_{-\infty}^{\infty}\frac{x(\zeta)}{\zeta - t}d\zeta$
FREQUENCY SHIFT	$\cos(\omega_m t)$	$\sin(\omega_m t)$
DOUBLE SIDEBAND	$x(t)$	0
TWO-TONE TEST	$2\cos(\omega_m t)$	0
PSK	$\cos\theta(t)$	$\sin\theta(t)$
QAM	$A(t)\cos\theta(t)$	$A(t)\sin\theta(t)$

The two tone signal is a simple double sideband waveform that is often used to characterize intermodulation distortion. The quadrature components of $z(t)$ can also be expressed as $x(t) = \rho(t)\cos\vartheta(t)$ and $y(t) = \rho(t)\sin\vartheta(t)$. An alternative representation of the bandpass signal is therefore

$$z(t) = \rho(t)\sin(\omega_{RF}t + \vartheta(t)) \tag{2}$$

#112111 - $15.00 USD Received 1 Jun 2009; revised 5 Aug 2009; accepted 13 Aug 2009; published 17 Aug 2009

The amplitudes are related by $\rho^2(t) = x^2(t) + y^2(t)$. It should be noted that this is more than a simple polar representation since $\rho(t)$ may take on a negative value. The two tone signal is one such example discussed below

3. Link description and transfer function

Figure 1 illustrates an optically-filtered phase-modulated analog photonic system considered in this paper. The output of a continuous wave (cw) laser at optical frequency Ω is split between the signal and the local oscillator (LO) paths. The signal path is phase modulated by an RF signal $z(t)$ centered at frequency ω_{RF}, while the LO path is phase modulated by a sinusoidal signal at frequency ω_{LO}. Along with the fundamental optical frequency numerous sideband frequency components are generated. These are the harmonics and intermodulation frequencies. The intermodulation frequencies are within the fundamental signal band and arise when the input RF signal consists of more than one frequency component. This occurs in the signal path, which is phase modulated with $z(t)$. Of these the third-order intermodulation distortion (TOI) is often dominant and limits the dynamic range. As shown in Fig. 1, the two phase modulated signals are combined and then optically filtered to reject the higher order harmonics. The bandwidth of the optical filter is 2Δ in order to retain just the first upper sideband of both the signals. At the receiver the LO signal is used to coherently downconvert to an intermediate frequency (IF) of ($\omega_{RF} - \omega_{LO}$) resulting in the signal $S(t)$ after balanced detection. We derive the expression for the recovered signal $S(t)$ in this E/O/E link.

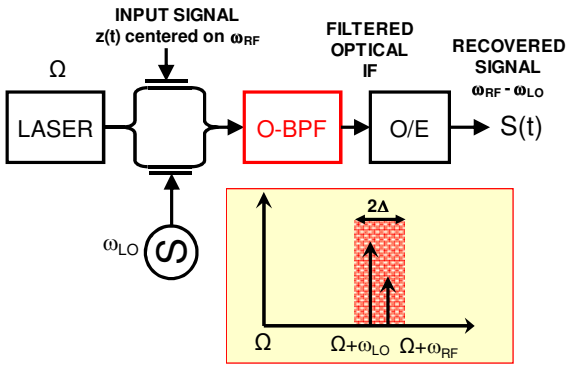

Fig. 1. Optically filtered analog photonic link.

The passband signal $z(t)$ expressed in terms of its two quadrature components $x(t)$ and $y(t)$ is given by Eq. (1).

The electrical field of the optical signal phase modulated with $z(t)$ is given by

$$E_M(t) \propto E_0 e^{j\beta z(t)} e^{j\Omega t} \tag{3}$$

Where $\beta = \pi / V_\pi$ is the phase modulator gain. V_π is the voltage required for a π phase shift. Substituting Eq. (2) in Eq. (3), the middle term can be expanded as a Bessel series

$$e^{j\beta\rho(t)\sin(\omega_{RF}t+\vartheta(t))} = \sum_{k=-\infty}^{+\infty} J_k(\beta\rho(t)) e^{jk(\omega_{RF}t+\vartheta(t))} \tag{4}$$

where $J_k(\cdot)$ is the k-th order Bessel function of the first-kind.

The optical filter rejects all components except the first upper sideband, for example. The filtered RF optical signal is coherently demodulated. The recovered signal $S(t)$ following coherent balanced detection with the LO optical signal is given by

$$S(t) \propto J_1(\beta\rho(t)) e^{j\vartheta(t)} e^{j(\omega_{RF}-\omega_{LO})t} \tag{5}$$

#112111 - $15.00 USD Received 1 Jun 2009; revised 5 Aug 2009; accepted 13 Aug 2009; published 17 Aug 2009

It is also possible to expand the phase modulation term in Eq. (3) explicitly in terms of the quadrature components $x(t)$ and $y(t)$. This leads to the product of two Bessel series in $i^k J_k(x)$ and $J_k(y)$ using

$$e^{j\beta x(t)\sin\theta} = \sum_{k=-\infty}^{+\infty} J_k(\beta x(t))\, e^{jk\theta} \tag{6}$$

$$e^{j\beta x(t)\cos\theta} = \sum_{k=-\infty}^{+\infty} J_k(\beta x(t))\, i^k\, e^{jk\theta} \tag{7}$$

Keeping all of the terms that contribute to the upper optical sideband, one would arrive at the expression

$$S(t) \propto e^{j(\omega_{RF}-\omega_{LO})t} \sum_p i^p J_{1-p}(\beta x(t))\, J_p(\beta y(t)) \tag{8}$$

One can see that Eq. (8) is completely equivalent to Eq. (5) using the Gegenbauer summation formula [9]:

$$\sum_{p=-\infty}^{+\infty} i^p\, J_{1-p}(\beta\rho(t)\cos\vartheta(t))\, J_p(\beta\rho(t)\sin\vartheta(t)) = J_1(\beta\rho(t))\, e^{i\vartheta(t)} \tag{9}$$

The phase modulated filtered response of the E/O/E link again reduces to the simple form given by Eq. (5).

Equation (5) gives the transfer function of the filtered phase-modulated link and shows that he recovered signal is a frequency translated and distorted version of the input RF signal. The amplitude modulation in Eq. (5) (or Eq. (9)) is given by $J_1\left(\beta\rho(t)\right) \approx \frac{1}{2}\beta\rho(t)$ and takes on both positive and negative values. From Eq. (5) the distortion can be described by

$$\frac{J_1(\beta\rho(t))}{\frac{1}{2}\beta\rho(t)} \cong 1 - \tfrac{1}{8}(\beta\rho(t))^2 + \tfrac{1}{192}(\beta\rho(t))^4 \tag{10}$$

This demonstrates that filtered phase-modulation produces envelope distortion. The envelope distortion depends on $\rho^2(t)$, which is positive valued and is independent of the phase $\vartheta(t)$.

The above analysis is valid for any kind of a passband signal $z(t)$. Next we apply it to two simpler cases of the RF modulating signal $z(t)$: single-tone and two-tone.

3.1 Case 1: Single-tone signal –invariance to frequency shift

We first consider the case when the modulating signal $z(t)$ is a pure single-tone at frequency $\omega_{RF} + \omega_m$ which can expressed as

$$\begin{aligned} z(t) &= x_0 \sin(\omega_{RF} + \omega_m)t \\ &= x_0 \sin(\omega_{RF}t)\cos(\omega_m t) + x_0 \cos(\omega_{RF}t)\sin(\omega_m t) \end{aligned} \tag{11}$$

where x_0 is the signal amplitude. The recovered signal $S(t)$ after optical filtering given by Eq. (5) (with $\rho(t) = x_0$) is simply shifted in frequency by ω_m with a constant amplitude $J_1(\beta x_0)$: there are no higher-order intermodulation terms, as expected.

3.2 Case 2: Two-tone signal – verify classical result

We next consider the simple two-tone signal with frequencies $\omega_{RF} \pm \omega_m$. As noted in Table 1, $z(t)$ in this case can be written as

$$z(t) = 2x_0 \cos(\omega_m t)\sin(\omega_{RF}t) \tag{12}$$

#112111 - $15.00 USD Received 1 Jun 2009; revised 5 Aug 2009; accepted 13 Aug 2009; published 17 Aug 2009

It is evident that $\rho(t) = 2x_0 \cos(\omega_m t)$ and $\vartheta(t) = 0$, for which Eq. (5) gives

$$S(t) = J_1\left(2\beta x_0 \cos(\omega_m t)\right) e^{i(\omega_{RF} - \omega_{LO})t} \tag{13}$$

The signal amplitude can be expanded using the Gegenbauer summation theorem to give

$$J_1\left(2\beta x_0 \cos(\omega_m t)\right) = \sum_{k=-\infty}^{\infty} (-1)^k J_k(\beta x_0) J_{k+1}(\beta x_0)\, e^{-i(2k+1)\omega_m t} \tag{14}$$

This indicates that the recovered signal $S(t)$ is centered around the IF ($\omega_{RF} - \omega_{LO}$) and consists of infinite frequency components at odd harmonics of ω_m. The fundamental is obtained at frequency ($\omega_{RF} - \omega_{LO}$) ± ω_m and has a magnitude $J_1(\beta x_0)J_0(\beta x_0)$, while the third-order intermodulation distortion at frequency ($\omega_{RF} - \omega_{LO}$) ± $3\omega_m$ has a magnitude of $J_2(\beta x_0)J_1(\beta x_0)$. These conclusions agree with the theory of two-tone signals well-known in literature.

4. Linearization techniques and experimental results

Distortion in passband filtered phase-modulated links appears as *envelope distortion* and can be mitigated either through feedforward correction which requires precise signal tracking or through post-compensation. In both cases the compensation response depends on the signal envelope rather than the carrier phase.

Using the link transfer function given by Eq. (5) we can readily implement predistortion or post-processing techniques for linearization. In predistortion the nonlinearity is compensated by pre-multiplying the RF modulating signal or the optical LO with the inverse of the nonlinearity.

Using post-processing, the distortion, produced by $J_1(\beta\rho(t))$, can be corrected when $\rho(t)$ is estimated from the observed waveform. One can determine $\rho(t)$ from measurements of $S(t)$ within the region where the slope of $J_1(\beta\rho(t))$ is nonzero using traditional digital signal processing (DSP) methods. Next we present experimental results on linearization based on post-processing. Experimental results on predistortion envelope compensation will be presented in a future publication. Furthermore, we have developed a novel technique based on multiscale sampling [10] to extend the inversion region beyond where the slope vanishes.

4.1 Experimental results

The experimental setup for a filtered E/O/E link with two-tones as the input RF modulating signal $z(t)$ is very similar to Fig. 1. The two-tones at frequencies 4.999 GHz and 5.001 GHz with ω_m = 1 MHz are passively combined and then amplified. The LO RF signal is at ω_{LO} = 5.055 GHz. The output power of a 1550nm laser with a linewidth of 100 KHz is input to a dual arm MZM. A narrow linewidth laser is essential to ensure that the noise floor is limited by shot noise rather than laser phase noise and phase noise decorrelated by narrow band optical filtering. One arm of the MZM is used for phase modulating the two-tone RF signal and the other arm is used for modulating the LO signal. This allows these two phase modulated signals to be coherently combined after which a narrowband filter with a 3-dB bandwidth of 350 MHz filters the upper sideband fundamental around 5 GHz. A bias is applied to the RF signal arm to suppress the strong optical carrier by more than 25dB. The filtered output is coherently detected resulting in the recovered signal $S(t)$ around an IF ω_{IF} = 55 MHz. This signal consists of the fundamental two tones (at $\omega_{IF} \pm \omega_m$) along with the intermodulation distortion terms of which the third-order (at $\omega_{IF} \pm 3\omega_m$) is dominant. Figure 2(a) shows the experimental time-domain recovered signal recorded at 5GSa/s using the Agilent 54853A real-time scope (8-bit resolution without averaging and 2.5 GHz bandwidth) for a high RF input power of 18.5 dBm and shows pronounced distortion. Equation (13) is fit to this data along with the envelope given by $J_1(2\beta\, x_0\cos(\omega_m t))$, showing excellent agreement and confirming the analysis derived above. This waveform will require multiscale sampling to invert the Bessel function and more details are found in reference [10].

#112111 - $15.00 USD Received 1 Jun 2009; revised 5 Aug 2009; accepted 13 Aug 2009; published 17 Aug 2009

The recovered passband signal envelope is slowly varying relative to ω_{IF}. The desired signal is given by $\rho(t)\sin(\omega_{IF}t + \theta)$ and can be reconstructed from measurements using

$$\left\langle S^2(t)\right\rangle = A_1^2\, J_1^2(\beta\rho(t)) \tag{15}$$

where $\left\langle S^2(t)\right\rangle = \int w(t-\xi)\, S(\xi)^2\, d\xi$, with A_1 as a constant and $w(t)$ as a low-pass window function over one cycle of the IF carrier. Finally $\rho(t)$ is reconstructed using

$$\rho(t) = \frac{1}{\beta} J_1^{-1}\left(\frac{\langle S\rangle}{A_1}\right) \tag{16}$$

The Bessel function is inverted using $J_1^{-1}(x) = 2x + 1.066941x^3 + 9.208205x^7 - 0.000056$ for $|\, x\,| \le 0.5$.

The IF output power of the fundamental and TOI are plotted as a function of the input RF power in Fig. 2 (b). The resulting fundamental and TOI after post-processing to correct the envelope distortion are also shown. It is seen that envelope distortion compensation significantly suppresses TOI by ~20dB. The improvement is limited by ADC resolution, numerical accuracy, higher order terms, and other sources of distortion, most prominently the RF amplifier distortion. Note that the post-compensation is less effective for high input RF powers (for example > 9dBm) as the inversion of the Bessel function is not accurate. Multiscale sampling would help to relieve this problem and thus extend the inversion region.

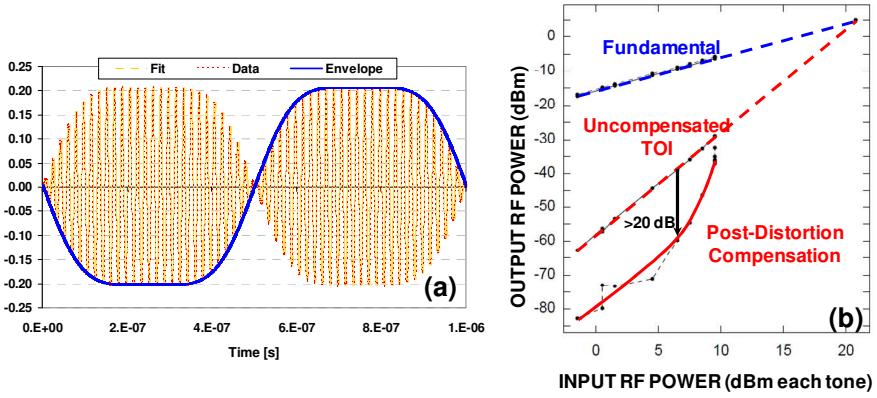

Fig. 2. Two-tone experimental data (a) Time-domain waveform along with a fit of the envelope. (b) Fundamental and TOI before and after post-processing.

Note that in addition to the suppression of TOI, the overall link linearity is also dependent on the link noise and bandwidth. This has been discussed in many of the referenced articles and in this paper we have focused on the suppression of TOI.

5. Summary

We have presented an analytical solution for the large signal transfer function of optically-filtered analog photonic systems such as those encountered in optical processing of RF signals. This solution is valid for *arbitrary* passband RF signals. It was shown that in filtered phase-modulated links the distortion appears as envelope distortion and can be compensated through predistortion and post-processing techniques that show promise for achieving high performance RF photonic links.

Acknowledgements

This material is based upon work supported by the Defense Advanced Research Projects Agency under Contract No. HR0011-08-C-0026.

#112111 - $15.00 USD Received 1 Jun 2009; revised 5 Aug 2009; accepted 13 Aug 2009; published 17 Aug 2009